SENSITIVITY OF OZONE CONCENTRATIONS TO RATE CONSTANTS IN A MODIFIED SAPRC90 CHEMICAL MECHANISM USED FOR CANADIAN LOWER FRASER VALLEY OZONE STUDIES

WEIMIN JIANG, DONALD L. SINGLETON, ROBERT McLAREN and MARK HEDLEY

Institute for Chemical Process and Environmental Technology, National Research Council Canada, Ottawa, Ont., Canada K1A 0R6

Abstract—The SAPRC90 chemical mechanism implemented in CALGRID is modified and updated for the specific emissions and applications of the Lower Fraser Valley (LFV) of British Columbia, Canada. Explicit reactions related to biogenic emissions and alternative fuels are added. The sensitivity of ozone formation to rate parameters in the mechanism is determined for an episode specific trajectory which originates under relatively clean marine conditions and passes over the urban core of Vancouver during the morning rush hour. Of the 137 reactions in the modified mechanism, the rate constants of 44 reactions are found to have a high sensitivity on ozone formation. The 44 reactions are further divided into general sensitive reactions, for which rate constant changes near the base case values have observable effects on maximum ozone concentrations, and limit-sensitive reactions, for which rate constant changes of more than an order of magnitude are required to have an observable impact on ozone concentrations. For the sensitive reactions, both ozone sensitivity coefficients for small changes (20%) in the rate constants and effects on ozone caused by large rate constant changes (factors of 0, 0.5, and 2) are calculated. Of note is the importance of several photolysis reactions and the reactions of OH with a class of reactive aromatics, including xylenes, on ozone concentrations in the LFV.

Key word index: Photochemical modelling, air pollution, smog, rate constants, sensitivity.

1. INTRODUCTION

Underprediction of ground-level ozone by photochemical models has been a problem facing the modelling community for some time. Among the factors that affect modelling results, poor emissions inventories are often cited as the most significant. Adjustments to the emissions inventories were often made based on emissions sensitivity tests in order to achieve good agreement between model outputs and the ambient measurements.

Another area that deserves more emphasis is the impact of uncertainties in the chemical mechanisms on the modelling results. The uncertainties exist in both the reactions used in the mechanisms and the rate constants of the reactions. As a key module in any photochemical modelling system, a chemical mechanism directly affects the modelling results. More attention needs to be paid to the sensitivity of modelling results to the chemical mechanisms and to the parameters in the chemical mechanisms in order to broaden our understanding.

This paper is focused on sensitivity of ozone concentrations to the rate constants of a modified version of the chemical mechanism implemented in the CALGRID model (Yamartino *et al.*, 1992), which is used in our three-dimensional (3D) modelling studies. It is based on the SAPRC90 mechanism (Carter, 1990). We added several explicit reactions relating to chemistry of biogenic emissions and emissions from the use of alternative fuels. To determine the sensitivities of ozone concentrations to the rate constants in the updated mechanism, the mechanism is incorporated into the OZIPR trajectory model (Gery and Crouse, 1989) to take advantage of OZIPR's high computational efficiency compared with grid models.

Sensitivities of kinetic parameters are calculated for a scenario in the Canadian Lower Fraser Valley (LFV). The LFV includes Vancouver, British Columbia, and the northern portion of Washington state. Ozone concentrations in the region during summer episodes frequently exceed the Canadian objective of 82 ppb (CCME, 1990). An episode-specific trajectory and emissions scenario of 18 July, 1985, is simulated, in which an air mass is constrained to pass over the urban core of Vancouver during the morning rush hour. The air mass, originating over the Strait of Georgia, is initially very clean, and ozone formation is

determined by the emissions as the air mass moves eastward through the LFV. In this respect, the analysis differs from other studies in which generalized meteorological or emission conditions are assumed, or in which the chemistry is based on initial concentrations of reactants without subsequent emissions. The reactions in the mechanism are classified into three categories according to the sensitivity of ozone concentrations to the rate constants. Because of the similarity of our tested mechanism with other versions of the SAPRC mechanism, the results presented here not only provide information for LFV ozone studies, but also enhance our understanding of the widely applied SAPRC mechanism.

2. DESCRIPTION OF THE CHEMICAL MECHANISM

2.1. *Original COND2243 mechanism*

CALGRID, obtained from the California Air Resources Board (CARB), was developed to upgrade and modernize the urban airshed model (UAM) by implementing state-of-the-science improvements in many of the key technical algorithms (Scire *et al.*, 1989). A recent version of CALGRID (version 1.5/S90, level 921130) contains a chemical mechanism named COND2243, which is a modified and lumped version of the SAPRC90 mechanism. The COND2243 mechanism contains 54 chemical species and 129 reactions. Among the 54 chemical species, there are two lumped alkanes, two lumped aromatics and three lumped olefins. The chemistry of methanol (MEOH), ethanol (ETOH), methyl *t*-butyl ether (MTBE) and methane (CH_4) are treated explicitly. Among the 129 chemical reactions, 16 are reactions of lumped VOC model species with OH, O_3, $O(^3P)$ and NO_3.

2.2. *Modification of the COND2243 mechanism*

The mechanism used in this study is a further modification to the COND2243 mechanism implemented in CALGRID. As a part of the Lower Fraser Valley ozone study, effects of alternative fuels and biogenic emissions on air quality will be evaluated. Therefore, methane (CH_4), propane (C_3H_8), methanol (MEOH), ethanol (ETOH), MTBE and isoprene (ISOP) reactions need to be presented explicitly in the chemical mechanism component of our models. Reactions for methacrolein (MACR) and methyl vinyl ketone (MVK), two key products of the isoprene reactions, are also needed.

For the chemistry of CH_4, MEOH and ETOH, we kept the explicit reactions in the COND2243 mechanism, and updated their rate constants to currently recommended values (Atkinson, 1994). For MTBE, we derived a new reaction based on the reaction sequence recommended by Atkinson (1994), which accounted for more complete reaction pathways than the original reaction in COND2243. In COND2243, C_3H_8 was lumped into an alkane group. In the present work, C_3H_8 was extracted from the alkane group and its reactions expressed explicitly using the mechanism of Carter (1990). Isoprene was treated as a regular alkene species in Carter (1990) and lumped into an alkene group in COND2243. Its explicit reactions, excluding ISOP + NO_3, and the reactions involving MACR and MVK were derived in the present work from more recent experimental results (Paulson *et al.*, 1992a, b; Paulson and Seinfeld, 1992; Aschmann and Atkinson, 1994; Grosjean *et al.*, 1993; Tuazon and Atkinson, 1990, 1989). Since there is no new experimental evidence to support a new reaction scheme for the ISOP + NO_3 reaction, the reaction used in Carter (1990) was adopted. Rate constants for all the above reactions are updated to the values recommended by Atkinson (1994). More detailed treatment of these reactions is available in Jiang *et al.* (1995).

The revised mechanism, named CD2273V2, is shown in Table 1. It contains 137 reactions and 64 model species. The updated explicit reactions discussed above are marked by reaction labels starting with "*". In these reactions, MEK, MFU3 and CHO_2 stand for methyl ethyl ketone, 3-methyl furan and thermally stabilized ·CH2OO· biradical, respectively; EPOX stands for epoxides

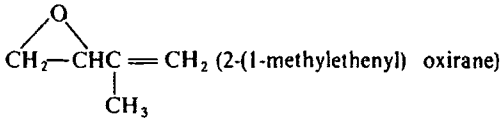

(2-(1-methylethenyl) oxirane)

and

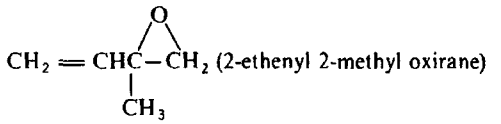

(2-ethenyl 2-methyl oxirane)

I3PR includes $CH_2 = C–C(O·)(CH_3)–CH_2O–O·$ and its three isomers; PPN is a surrogate model species that is used to represent higher PAN analogues. In addition to the modification described above, rate constants and product yields of lumped VOC reactions as well as carbon numbers and molecular weights of the lumped VOC species are recalculated and updated using the speciation profile of the LFV emissions. The speciated emissions profile contains mass emissions of 574 emitted VOC classes, identified by their SAROAD (Storage and Retrieval of Aerometric Data) numbers, in the LFV modelling domain. The profile reflects the emissions characteristics of the region, and the recalculated parameters based on the profile reflect the region-specific feature of some mechanism parameters. The photolysis rates in the mechanism are recalculated for all reactions for which data are given by Carter (1990), using absorption coefficients and quantum yields given by Carter (1990) and actinic fluxes given by Finlayson-Pitts and Pitts (1986). This included nearly all the photolysis reactions.

Table 1. The CD2273V2 mechanism[a–d]

Label[e]	Reaction	A (cm molec sec)	B	E_a/R (K)
1G	$NO_2 + h\nu = NO + O$	Phtol		
2L	$O + O_2 + M = O_3 \{ + M\}$	6.000E-34	−2.3	
3	$O + NO_2 = NO \{ + O_2\}$	6.5000E-12		−119.8
4	$O + NO_2 = NO_3 \{ + M\}$	9.0E-32	2.0	
		2.2E-11		
5G	$NO + O_3 = NO_2 \{ + O_2\}$	2.0E-12		1400.0
6	$NO_2 + O_3 = NO_3 \{ + O_2\}$	1.4E-13		2500.0
7	$NO + NO_3 = 2*NO_2$	1.7E-11		−150.0
8	$NO + NO + O_2 = 2*NO_2$	3.3E-39		−528.4
9	$NO_2 + NO_3 = N_2O_5$	2.2E-30	−4.3	
		1.5E-12	−0.5	
10	$N_2O_5 = NO_2 + NO_3$	k_9/1.01E-27 exp(11202/T)		
11	$N_2O_5 + H_2O = 2*HNO_3$	1.0000E-21		
12	$NO_2 + NO_3 = NO + NO_2 \{ + O_2\}$	2.5000E-14		1227.9
13	$NO_3 + h\nu = NO \{ + O_2\}$	Phto2		
14	$NO_3 + h\nu = NO_2 + O$	Phto3		
15	$O_3 + h\nu = O \{ + O_2\}$	Phto4		
16G	$O_3 + h\nu = O1D \{ + O_2\}$	Phto5		
17G	$O1D + H_2O = 2*OH$	2.200E-10		
18G	$O1D + M = O \{ + M\}$	1.92E-11		−126.3
19	$NO + OH = HONO$	7.0E-31	−2.6	
		1.5E-11	−0.5	
20L	$HONO + h\nu = NO + OH$	Phto6		
21G	$NO_2 + OH = HNO_3$	2.6E-30	−3.2	
		2.4E-11	−1.3	
22	$HNO_3 + OH = NO_3 + H_2O$	6.45E-15		−831.3
23	$HNO_3 + h\nu = OH + NO_2$	Phto7		
24G	$CO + OH = HO_2 \{ + CO_2\}$	2.4E-13		
25	$O_3 + OH = HO_2 \{ + O_2\}$	1.6002E-12		942.0
26L	$NO + HO_2 = NO_2 + OH$	3.7E-12		−241.5
27	$NO_2 + HO_2 = HNO_4$	1.8E-31	−3.2	
		4.7E-12	−1.4	
28L	$HNO_4 = NO_2 + HO_2$	k_{27}/2.1E-27 exp(10900/T)		
29	$HNO_4 + OH = NO_2 + H_2O \{ + O_2\}$	1.3E-12		−379.9
30	$O_3 + HO_2 = OH \{ + 2*O_2\}$	1.1E-14		500.2
31	$HO_2 + HO_2 = H_2O_2 \{ + O_2\}$	2.20E-13		−619
32	$HO_2 + HO_2 + M = H_2O_2 \{ + O_2\}$	1.90E-33		−981
33	$HO_2 + HO_2 + H_2O = H_2O_2 \{ + O_2\} + H_2O$	3.10E-34		−2818
34	$HO_2 + HO_2 + H_2O = H_2O_2 \{ + O_2\} + H_2O$	6.60E-35		−3181
35	$NO_3 + HO_2 = HNO_3 \{ + O_2\}$	k_{31}		
36	$NO_3 + HO_2 + M = HNO_3 \{ + O_2\}$	k_{32}		
37	$NO_3 + HO_2 + H_2O = HNO_3 \{ + O_2\} + H_2O$	k_{33}		
38	$NO_3 + HO_2 + H_2O = HNO_3 \{ + O_2\} + H_2O$	k_{34}		
39	$H_2O_2 + h\nu = 2*OH$	Phto8		
40	$H_2O_2 + OH = HO_2 + H_2O$	3.3E-12		199.8
41	$OH + HO_2 = H_2O \{ + O_2\}$	4.6E-11		−230
42	$SO_2 + OH = HO_2 + SULF$	3.0E-31	−3.3	
		1.5E-12		
43	$O_3SB + H_2O =$	2.3E-17		
44	$O_3SB + SO_2 = SULF$	1.0E-13		
45	$RO_2 + NO = NO$	4.2E-12		−181.2
46	$RO_2 + HO_2 = HO_2$	3.4E-13		−800.1
47	$RO_2 + RO_2 =$	1.0E-15		
48	$RO_2 + C_2O_3 = C_2O_3$	1.86E-12		−529.9
49	$RO_2 + C_3O_3 = C_3O_3$	1.86E-12		−529.9
50L	$RO_2R + NO = NO_2 + HO_2$	4.2E-12		−181.2
51	$RO_2R + HO_2 = ROOH$	3.4E-13		−800.1
52	$RO_2R + RO_2 = 0.5*HO_2 + RO_2$	1.0E-15		
53	$RO_2R + C_2O_3 = HO_2 + HCHO + CO_2$	1.86E-12		−529.9
54	$RO_2R + C_3O_3 = HO_2 + CCHO + CO_2$	1.86E-12		−529.9
55L	$RO_2N + NO = RNO_3$	4.2E-12		−181.2
56	$RO_2N + HO_2 = ROOH + MEK + 1.5*C$	3.4E-13		−800.1
57	$RO_2N + RO_2 = RO_2 + 0.5*HO_2 + MEK + 1.5*C$	1.0E-15		
58	$RO_2N + C_2O_3 = HO_2 + HCHO + MEK + 1.5*C$	1.86E-12		−529.9
59	$RO_2N + C_3O_3 = HO_2 + CCHO + MEK + 1.5*C$	1.86E-12		−529.9
60L	$R_2O_2 + NO = NO_2$	4.2E-12		−181.2
61	$R_2O_2 + HO_2 =$	3.4E-13		−800.1
62	$R_2O_2 + RO_2 = RO_2$	1.0E-15		
63	$R_2O_2 + C_2O_3 = 0.5*HO_2 + HCHO + CO_2$	1.86E-12		−529.9
64	$R_2O_2 + C_3O_3 = 0.5*HO_2 + CCHO + CO_2$	1.86E-12		−529.9
65	$ROOH + h\nu = HO_2 + OH$	Phto9		
66	$OH + ROOH = OH$	1.18E-12		−127.8
67	$OH + ROOH = RO_2R + RO_2$	1.79E-12		−218.9
68G	$HCHO + h\nu = 2*HO_2 + CO$	Phto10		
69G	$HCHO + h\nu = CO$	Phto11		
70G	$HCHO + OH = HO_2 + CO + H_2O$	1.125E-12	2.0	−648.1
71	$HCHO + HO_2 = HOCOO$	9.70E-15		−625
72	$HOCOO = HO_2 + HCHO$	2.4E12		7001

Table 1. (Continued)

Label[c]	Reaction	A (cm molec sec)	B	E_a/R (K)
73	$HOCOO + NO = NO_2 + HO_2 + C$	4.2E-12		− 181.2
74	$HCHO + NO_3 = HNO_3 + HO_2 + CO$	2.8E-12		2516.4
75G	$CCHO + OH = C_2O_3 + H_2O$	5.55E-12		− 311.0
76G	$CCHO + h\nu = CO + HCHO + HO_2 + RO_2R + RO_2$	Phto12		
77	$CCHO + NO_3 = HNO_3 + C_2O_3$	1.4E-12		1860.0
78	$RCHO + OH = C_3O_3$	8.5E-12		− 251.6
79G	$RCHO + h\nu = CCHO + HO_2 + CO + RO_2R + RO_2$	Phto13		
80	$RCHO + NO_3 = HNO_3 + C_3O_3$	1.4E-12		1860.0
81G	$MEK + OH = H_2O + 1.5*RO_2 + 1.5*R_2O_2 + 0.5*CCHO + 0.5*C_3O_3 + 0.5*HCHO + 0.5*C_2O_3$	2.92E-13		− 414.2
82G	$MEK + h\nu = C_2O_3 + CCHO + RO_2R + RO_2$	Phto14		
83	$RNO_3 + OH = NO_2 + 0.155*MEK + 1.05*RCHO + 0.48*CCHO + 0.16*HCHO + 1.39*R_2O_2 + 1.39*RO_2 + 0.11*C$	2.191E-11		708.6
84G	$C_2O_3 + NO = CO_2 + NO_2 + HCHO + RO_2R + RO_2$	5.10E-12		− 199.8
85G	$C_2O_3 + NO_2 = PAN$	1.95E-28	− 4.0	
		8.40E-12		
		$F = 0.27$	$n = 1.0$	
86	$C_2O_3 + HO_2 = ROOH + HCHO + CO_2$	3.4E-13		− 800.2
87	$C_2O_3 + C_2O_3 = 2.0*HO_2 + 2.0*HCHO + 2.0*CO_2$	2.8E-12		− 529.9
88	$C_2O_3 + C_3O_3 = 2.0*HO_2 + HCHO + CCHO + 2.0*CO_2$	2.8E-12		− 529.9
89G	$PAN = C_2O_3 + NO_2$	6.30E-2		12786
		2.2E16		13436
		$F = 0.27$	$n = 1.0$	
90G	$C_3O_3 + NO = CO_2 + NO_2 + CCHO + RO_2R + RO_2$	5.10E-12		− 199.8
91G	$C_3O_3 + NO_2 = PPN$	8.40E-12		
92	$C_3O_3 + HO_2 = ROOH + CCHO + CO_2$	3.4E-13		− 800.2
93	$C_3O_3 + C_3O_3 = 2.0*HO_2 + 2.0*CCHO + 2.0*CO_2$	2.8E-12		− 529.9
94G	$PPN = C_3O_3 + NO_2$	1.6E17		14074
95G	$CRES + OH = 0.15*RO_2N + 0.075*CRES + 0.85*RO2R + 0.2*MGLY + RO_2 + 5.5*C$	4.2E-11		
96	$CRES + NO_3 = HNO_3 + BZO + C$	2.1E-11		
97	$MGLY + h\nu = HO_2 + CO + C_2O_3$	Phto 15		
98G	$MGLY + h\nu = HO_2 + CO + C_2O_3$	0.107 × Phto 16		
99G	$MGLY + OH = CO + C_2O_3$	1.72E-11		
100	$MGLY + NO_3 = HNO_3 + CO + C_2O_3$	1.4E-12		1860
101	$BZO + NO_2 = RNO_3 + 0.5*CRES + -2.5*C$	1.3E-11		− 300.0
102	$BZO + HO_2 = 0.5*CRES + -2.5*C$	3.4E-13		− 800.1
103	$BZO = 0.5*CRES + -2.5*C$	1.0E-3		
104G	$AFG2 + OH = C_3O_3$	1.72E-11		
105G	$AFG2 + h\nu = HO_2 + CO + C_2O_3$	Phto 17		
*106G	$CH_4 + OH = HCHO + RO2R + RO_2$	6.696E-13	2.0	1361
107G	$ALK1 + OH = 0.8856*RO2R + 0.0856*RO2N + 0.0288*HO_2 + 0.5457*R_2O_2 + 1.5169*RO_2 + 0.0695*HCHO + 0.3230*CCHO + 0.1956*RCHO + 0.5948*MEK$ $0.0066*CO + 0.0650*C$	3.597E-12		
108G	$ALK2 + OH = 0.7639*RO_2R + 0.2102*RO_2N + 0.0259*HO_2 + 0.8401*R_2O_2 + 1.8142*RO_2 + 0.1337*HCHO + 0.0797*CCHO + 0.3203*RCHO + 0.9581*MEK + 0.03441*CO + 0.0339*CO_2 + 1.3235*C$	1.2967E-11		
109G	$ETHE + OH = 0.22*CCHO + 1.56*HCHO + RO_2R + RO_2$	1.96E-12		− 437.8
110	$ETHE + O_3 = HCHO + 0.37*O_3SB + 0.12*HO_2 + 0.44*CO + 0.56*C$	1.2E-14		2630.0
111	$ETHE + O = HCHO + HO_2 + CO + RO_2R + RO_2$	1.04E-11		792.0
112	$ETHE + NO_3 = NO_2 + 2*HCHO + R_2O_2 + RO_2$	1.96E-12		2724.0
113G	$OLE1 + OH = 0.9660*HCHO + 0.5301*CCHO + 0.2787*RCHO + 0.0629*MEK + 0.9660*RO_2R + 0.0340*RO_2N + RO_2 + 0.5777*C$	3.1829E-11		
114	$OLE1 + O_3 = 0.5823*HCHO + 0.3177*CCHO + 0.1442*RCHO + 0.2351*MEK + 0.0163*MGLY + 0.2828*CO + 0.2687*O_3SB + 0.1479*HO_2 + 0.0665*OH + 0.1293*RO_2R + 0.1293*RO_2 + 0.9392*C$	1.1827E-17		
115	$OLE1 + O = 0.4*HO_2 + 0.5*MEK + 0.5*RCHO + 2.1114*C$	5.8620E-12		
116	$OLE1 + NO_3 = NO_2 + HCHO + 0.5488*CCHO + 0.2885*RCHO + 0.0651*MEK + R_2O_2 + RO_2 + 0.6381*C$	6.0223E-14		
117	$OLE2 + OH = 0.1570*HCHO + 0.7837*CCHO + 0.7232*RCHO + 0.0721*MEK + 0.9365*RO_2R + 0.635*RO_2N + RO_2 + 0.4097*C$	6.5558E-11		
118G	$OLE2 + O_3 = 0.2111*HCHO + 0.5360*CCHO + 0.3861*RCHO + 0.3577*MEK + 0.0108*MGLY + 0.1576*CO + 0.1919*O_3SB + 0.0017*C_2O_3 + 0.0017*C_3O_3 + 0.1790*HO_2 + 0.1107*OH + 0.2280*RO_2R + 0.0051*R_2O_2 + 0.2331*RO_2 + 0.8393*C$	2.0250E-16		
119	$OLE2 + O = 0.4*HO_2 + 0.5*MEK + 0.5*RCHO + 3.1597*C$	2.5142E-11		
120	$OLE2 + NO_3 = NO_2 + 0.1677*HCHO + 0.8369*CCHO + 0.7722*RCHO + 0.0770*MEK + R_2O_2 + RO_2 + 0.4436*C$	1.3116E-12		
121G	$OLE3 + OH = 0.4754*HCHO + RCHO + RO_2R + RO_2 + 5.0708*C$	7.0909E-11		

Table 1. (Continued)

Label[c]	Reaction	A (cm molec sec)	B	E_a/R (K)
122	OLE3 + O_3 = 0.2377•HCHO + 0.15•CCHO + 0.5•RCHO + 0.21•MEK + 0.1796•CO + 0.1880•O_3SB + 0.1335•HO_2 + 0.06•OH + 0.135•RO_2R + 0.135•RO_2 + 5.4889•C	5.2483E-17		
123	OLE3 + O = 0.4•HO_2 + 0.5•MEK + 0.5•RCHO + 6.7962•C	3.8394E-11		
124	OLE3 + NO_3 = NO_2 + 0.4754•HCHO + RCHO + R_2O_2 + RO_2 + 5.0708•C	3.6625E-12		
125G	ARO1 + OH = 0.7433•RO_2R + 0.2567•HO_2 + 0.7433•RO_2 + 0.2567•CRES + 0.1132•MGLY + 0.3603•AFG2 + 3.9982•C	5.869E-12		
126G	ARO2 + OH = 0.8176•RO_2R + 0.0051•RO_2N + 0.1773•HO_2 + 0.8228•RO_2 + 0.1798•CRES + 0.4310•MGLY + 0.6061•AFG2 + 4.2979•C	2.7279E-11		
*127	MEOH + OH = HCHO + HO_2	5.4091E-13	2.0	− 170.0
*128	ETOH + OH = HO_2 + CCHO	5.5620E-13	2.0	− 532.0
*129	MTBE + OH = RO_2R + 0.42•R_2O_2 + 1.42•RO_2 + 0.48HCHO + 0.76•RCHO + 0.204•MEK + 1.34•C	5.886E-13	2.0	− 483.14
*130G	ISOP + OH = ISOH	2.54E-11		− 410.17
*131L	ISOH + NO = 0.41•MACR + 0.41•MVK + 0.605•HCHO + 0.14•RNO_3 + 0.04•MFU_3 + 0.86•HO_2 + 0.86•NO_2	4.9E-12		− 180.17
*132	ISOP + O_3 = 0.59•MACR + 0.16•MVK + 0.89•HCHO + 0.27•OH + 0.27•HO_2 + 0.30•O + 0.40•RO_2 + 0.40•R_2O_2 + 0.27•CO + 0.05•EPOX + 0.38•CHO_2 + 0.27•CO_2	7.86E-15		1913
*133	ISOP + NO_3 = NO_2 + HCHO + RCHO + R_2O_2 + RO_2	3.3E-12		445.9
*134	ISOP + O = 0.85•EPOX + 0.085•I_3PR	5.8E-11		
*135	MACR + OH = 0.16•MEK + 0.51•CO + 0.084•MGLY + 0.56•HCHO + 1.48•RO_2 + 0.68•RO_2R + 0.18•R_2O_2 + 0.12•PAN + 0.2•PPN + 0.48•CO_2	1.86E-11		− 175.14
*136	MVK + OH = 0.64•CCHO + 0.26•MGLY + 0.52•HCHO + 0.1•RO_2N + 1.92•RO_2 + 0.52•RO_2R + 0.90•R_2O_2 + 0.38•PAN + 0.26•CO_2	4.13E-12		− 451.94
*137	C_3H_8 + OH = 0.9612•RO_2R + 0.0388•RO_2N + RO_2 + 0.26337•MEK + 0.30277•RCHO	1.350E-12	2.0	44.0

[a] $k = A \times (T/300)^B \times e^{-E_a/RT}$ unless discussed in other footnotes; all rate constants are in cm molec s units.

[b] "Phto 1" stands for photolysis rate set 1, and so on. The photolysis rate sets are omitted for simplicity and are available upon request.

[c] If more than one line appears for a rate constant, the rate constant is calculated by

$$k = \left(\frac{k_0[M]}{1 + k_0[M]/k_i}\right) F^G \quad \text{where } k_0 = A_0 \times \left(\frac{T}{300}\right)^B \times e^{-C_0/T},$$

$$k_i = A \times \left(T/300\right)^{B_i} \times e^{-C_i/T}, \quad G = \frac{1}{1 + [(\log k_0[M]/k_i)/n]^2}.$$

The first line in the table gives A_0, B_0, C_0; the second line gives A_i, B_i, C_i; and the third line gives F and n. If the third line is omitted, then $F = 0.6$, $n = 1.0$.

[d] Some rate constants are derived from the rate constants of other reactions using formulas specified in the table.

[e] Reaction labels: "*" indicates an updated reaction; numbers show the sequential numbers of the reactions; "G" and "L" stand for general-sensitive and limit-sensitive reactions, respectively, as discussed in the text. Reaction labels without "G" or "L" indicate non-sensitive reactions.

In the process of chemical mechanism modification and emissions processing, Carter's mechanism preparation software package (Carter, 1988) and U.S. EPA's Emissions Processing System 2 (EPS2) (Gardner *et al.*, 1992) are used. Minor modifications to Carter's programs are made to reconcile the software packages and our modelling system.

3. SENSITIVITY OF OZONE CONCENTRATIONS TO THE RATE CONSTANTS OF THE CD2273V2 MECHANISM

The OZIPR trajectory model (Gery and Crouse, 1989) is used to study sensitivity of ozone concentrations to the rate constants of the CD2273V2 mechanism for conditions of an ozone episode in the LFV. OZIPR is a research-oriented version of EPA's OZIPP (Ozone Isopleth Plotting Package) computer modelling program. It has enhanced input–output capability compared to OZIPP. As a trajectory model, OZIPR simulates chemical and physical processes of an air column moving along the wind trajectory. Emissions are injected into the air column as the column passes over emission sources. Air above the column is mixed in as the mixing height rises during the day.

3.1. *Input to the OZIPR trajectory model*

The input to the OZIPR model includes initial concentrations in the mixed and aloft layers and hourly emissions, mixing heights, humidity, and temperature. The meteorological and chemical emissions were based on input data for one day of the 17–21 July 1985, episode that we are simulating with the MC2 meteorological model (Tanguay *et al.*, 1990) and CALGRID photochemical model (Yamartino *et al.*, 1992). For 18 July 1985, a trajectory was obtained using MC2 and other software. It was constrained to

pass over the urban core of Vancouver at 8:00 during the morning rush hour. The trajectory starts at 6:00 a.m. over the ocean about 15 km west of the coast. After passing over Vancouver, it continues in a generally easterly direction, travelling over forested areas at the end of the day. The trajectory and the LFV modelling region are shown in Fig. 1. Meteorological conditions, including the hourly mixing height, temperature, and humidity, were taken from the corresponding grids of the MC2 simulation.

The hourly emissions into the air mass were taken from an episode specific emissions inventory for 18 July 1985. The emissions inventory was based on the Lower Mainland Emissions Inventory in British Columbia and an inventory of sources in Whatcom County in Washington state (McLaren *et al.*, 1995). It was processed to obtain hourly speciated emissions on a 5×5 km^2 grid. The emissions from each grid entering the moving air mass along the trajectory, assumed to have horizontal dimensions of 20×20 km^2, were weighted by the extent of coverage by the air mass. For the last two hours of the simulation, the air mass moves outside the boundary of the anthropogenic emissions inventory into a predominantly forested region, which is assumed to have only biogenic emissions. The organic compound emissions are respeciated to accommodate the modifications in the chemical mechanism and to match the speciation profile of the LFV emissions. The hourly speciated emissions along the trajectory are shown in Fig. 2. The hourly meterological and chemical emissions data are given in Table 2.

Since the air mass started over the ocean in the early morning, it is assumed that the air mass was very clean. The assumed initial ground-level concentrations were: O_3 15 ppb; VOC 10 ppbC; NO_x 1 ppb; CO 200 ppb. The initial aloft concentrations were: O_3 20 ppb; VOC 20 ppbC; NO_x 2 ppb; CO 200 ppb. The assumed initial ground-level concentrations are consistent with typical observed concentration ranges for regions between remote marine sites and urban sites (NRC, 1991; Chameides *et al.*, 1992). The NO_x and VOC concentrations were interpolated values between the remote marine sites and the urban sites. The O_3 concentration is set at the lower end of the marine site O_3 range. The CO concentration of 200 ppb is the typical value for remote areas (Finlayson-Pitts and Pitts, 1986). The assumed initial concentrations of O_3, NO_x, CO and VOC are consistent with the surface-level concentrations of 16 ppb, 2.9 ppb, 232 ppb, and 46 ppbC, respectively, calculated with MC2-CALGRID for the corresponding grid cells and time. The initial CH_4 concentration is set to the global background value of 1.79 ppm. Speciation of the initial VOC is based on the average VOC emissions in our modelling domain. Since the initial air mass is clean, any difference in model results caused by alternative speciation of initial VOC would be very small.

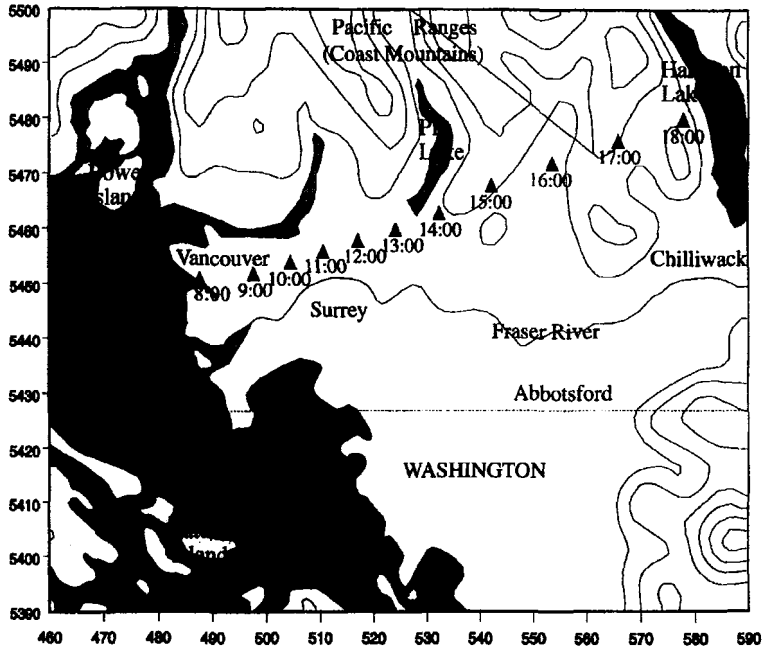

Fig. 1. The Lower Fraser Valley (LFV) modelling region. The selected air mass trajectory for the period 6:00–18:00, 18 July 1985 is shown by a series of black triangles. Numbers on the horizontal and vertical axis are UTM (Universal Transverse Mercator) coordinates in km (in UTM zone 10).

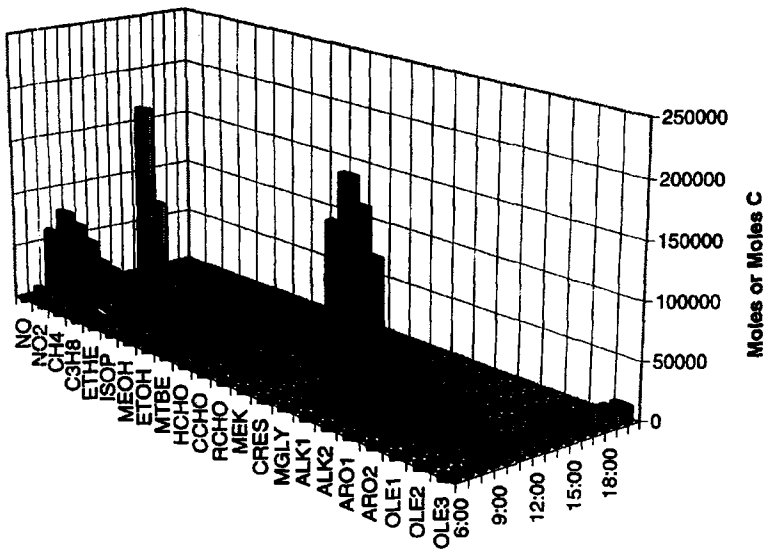

Fig. 2. Hourly emissions entering the moving air mass. Units for the emitted NO_x and VOC model species are "mol" and "mol C", respectively.

Table 2. Hourly mixing height, temperature, relative humidity, and VOC and NO_x emissions along the trajectory

Hour	MH (m)	T (K)	RH (%)	VOC (mol C)	NO_x (mol)
6:00	100.0	291	72	403	104
7:00	98.9	292	73	50,473	7672
8:00	457.9	294	71	421,974	67,533
9:00	440.4	295	70	523,243	86,284
10:00	448.7	297	68	426,654	69,799
11:00	470.9	298	66	295,773	48,547
12:00	542.2	299	38	150,343	23,774
13:00	617.7	299	37	249,060	9093
14:00	669.8	299	34	127,663	1980
15:00	697.1	299	32	31,929	20
16:00	709.2	299	27	23,301	0
17:00	735.8	300	28	22,355	0
18:00	616.1	299	28	14,195	0
19:00	564.8	298	32	14,195	0
20:00	513.4	297	36	14,195	0
21:00	462.0	296	40	14,195	0
22:00	410.7	295	44	14,195	0

3.2. *Reaction classification based on sensitivity of ozone concentrations to the rate constants*

To test the sensitivity of O_3 concentrations to rate constants, each rate constant in the CD2273V2 mechanism is multiplied by a factor ranging from 0 to 2.0 with an interval of 0.5. Particular attention is paid to the difference between the O_3 responses to zero rate constant and to non-zero rate constants.

O_3 concentrations respond very differently to rate constant changes of different reactions in the CD2273V2 mechanism. For some reactions, the O_3 concentrations do not change at all (to within 0.1 ppb) when their rate constants are changed from zero to two times their base case values. For some other reactions, maximum 1 h average O_3 concentrations can vary as much as 362 ppb for the same rate constant range mentioned above. To differentiate the reactions according to their sensitivities, we use 2% as a standard. A reaction is classified as a sensitive reaction if the maximum one hour average O_3 varies more than 2% of the base case value when the rate constant is changed from zero to twice the base case value. All other reactions are classified as non-sensitive reactions.

Among the 137 reactions in the CD2273V2 mechanism, 44 of them are found to be sensitive reactions. The other 93 reactions are non-sensitive. Among the 44 sensitive reactions, 8 are classified as limit-sensitive reactions because very large changes in the rate constant, for example, setting it to zero, are required before significant changes are made on ozone concentrations. The remaining 36 reactions are termed general sensitive reactions. The difference between the two types of reactions can be seen in the following sections.

3.2.1. *General sensitive reactions.* The most important example of general ozone sensitive reactions is the photolysis of NO_2. This is the only reaction that leads to the formation of ground state O and photochemical O_3. Figure 3a shows the O_3 concentration curves corresponding to different rate constants of the NO_2 photolysis reaction. When the rate constant is doubled, the maximum 1 h average O_3 concentration reaches 91.2 ppb, which is 22% higher than the base case O_3 concentration. When the rate constant drops to half of its base case value, the O_3 concentration drops by 29% to 45.9 ppb. As we will show in Section 3.3, the sensitivity of maximum O_3 concentrations to changes in base case NO_2 photolysis rate is the highest among all 137 reactions.

High sensitivity of O_3 concentrations to the NO_2 photolysis rates suggests that the NO_2 supply in the system is abundant enough and one of the limiting factors in O_3 production is the photolysis rate constant. It also suggests the potential for O_3 in the LFV to reach higher levels if actinic flux were to increase.

Another typical O_3 sensitive reaction is Reaction 16, which is the photolysis of O_3 into excited state $O(^1D)$ and O_2. Curves of instantaneous O_3 concentrations using different rate constants are shown in

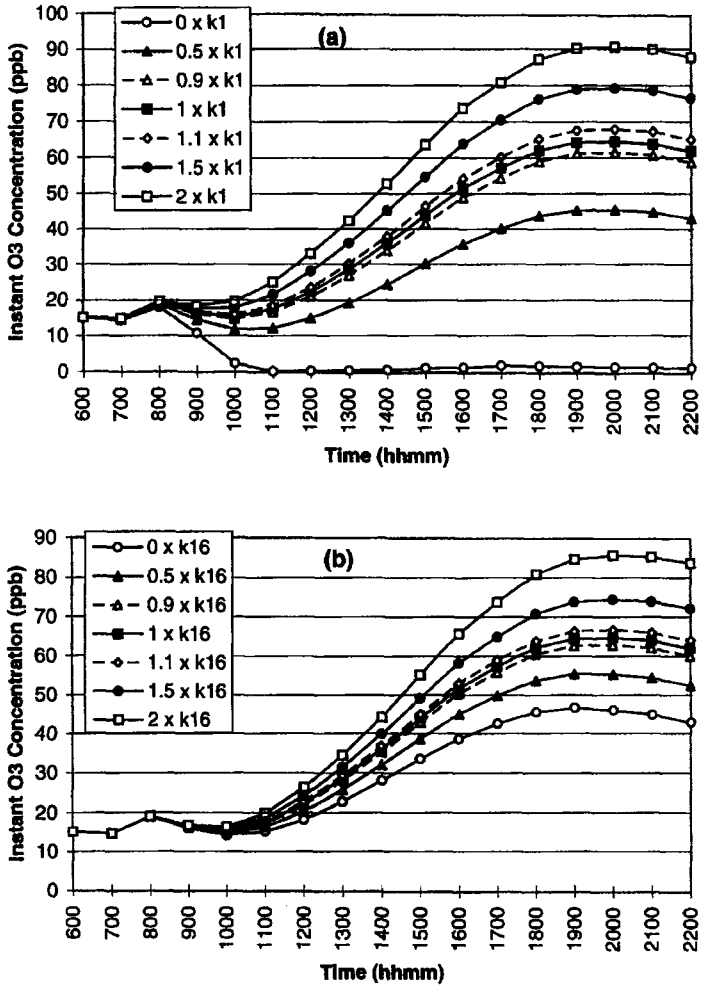

Fig. 3. Examples of sensitivities of O_3 concentrations to rate constants of general sensitive reactions. (a) O_3 sensitivities to k_1, which is the rate constant for NO_2 photolysis; (b) O_3 sensitivities to k_{16}, which is the rate constant for $O_3 + h\nu = O(^1D) + O_2$. On the legend, "$0.5 \times k1$" stands for base case k_1 values multiplied by 0.5, and so on.

Fig. 3b for the reaction. When the rate constant is lowered to half of the base case value, the maximum 1 h average O_3 concentration drops to 55.6 ppb from a base value of 64.9 ppb. When the rate constant is lowered to zero, the maximum 1 h average O_3 concentration becomes 46.8 ppb. Doubling the rate constant raises the maximum 1 h average O_3 concentration to 85.8 ppb. In Section 3.3, we will show that the sensitivity of maximum O_3 concentrations to the changes in the base case O_3 photolysis rate is the third highest among all 137 reactions.

The 36 general sensitive reactions are shown in Table 1 by reaction labels ended with the letter "G".

3.2.2. *Limit-sensitive reactions.* Within the 44 sensitive reactions, there is a subcategory of eight reactions that exhibit anomalous sensitivity. When a rate constant in this subcategory is multiplied by a factor ranging from 0.5 to 2, O_3 concentration changes are hardly noticeable (less than 1 ppb). However, when the rate constant is dropped to zero, which is equivalent to eliminating the reaction, dramatic changes in O_3 concentrations appear. The 8 reactions in this subcategory are Reactions 2, 20, 26, 28, 50, 55, 60 and 131. Reaction labels ending with "L" are used for these reactions in Table 1.

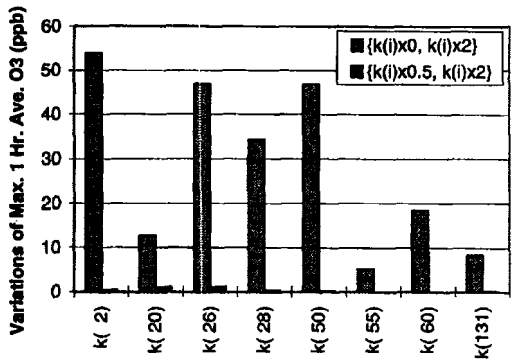

Fig. 4. Comparison of the variations of maximum 1 h average O_3 in the rate constant range $k \times 0.5$ to $k \times 2$ with those in the rate constant range $k \times 0$ to $k \times 2$ for the limit-sensitive reactions. $\{k(i) \times 0, k(i) \times 2\}$ stands for the O_3 variation in the range $k_i \times 0$ to $k_i \times 2$ while $\{k(i) \times 0.5, k(i) \times 2\}$ stands for the O_3 variation in the range $k_i \times 0.5$ to $k_i \times 2$.

Comparison of variations of maximum 1 h average O_3 in two different rate constant ranges for the reactions is shown in Fig. 4. In the figure, $\{k(i) \times 0.5, k(i) \times 2\}$ stands for the O_3 variation in the rate constant range $k \times 0.5$ to $k \times 2$ for the ith reaction while $\{k(i) \times 0, k(i) \times 2\}$ stands for the O_3 variation in the range $k(i) \times 0$ to $k(i) \times 2$. The O_3 variations in the rate constant range $k \times 0.5$ to $k \times 2$ are nearly imperceptible in the figure, but the O_3 variations in the range $k \times 0$ to $k \times 2$ are very obvious. For all these reactions, only a very small fraction (less than 10%) of the O_3 variations in the $k \times 0$ to $k \times 2$ range appears in the $k \times 0.5$ to $k \times 2$ range. That is to say, the O_3 concentrations are not sensitive to rate constant changes near the base case value. They become sensitive only when the rate constants approach the limit value of zero. Therefore, the 8 reactions are classified as limit-sensitive reactions to indicate their O_3 sensitivity near zero rate constant values. More than an order of magnitude reduction in their rate constants is needed in order to see meaningful changes in ozone concentrations. These reactions are interesting since they are required in the mechanism although the sensitivity of ozone concentrations to small changes in the base case rate constants is negligible

Reaction 50, $RO2R\cdot + NO = NO_2 + HO_2\cdot$, is a representative of this type of reaction. Seven O_3 concentration curves corresponding to $k_{50} \times 0$, 0.5, 0.9, 1.0, 1.1, 1.5, 2.0 are shown in Fig. 5. However, only two curves are apparent since all non-zero rate constant curves overlap each other. The dramatic drop in O_3 concentrations when the rate constant is reduced to 0 indicates that the reaction is limit-sensitive. The

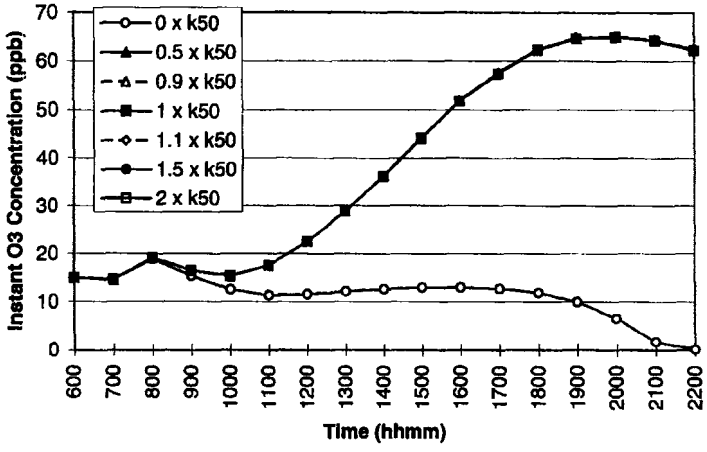

Fig. 5. Sensitivity of O_3 concentrations to rate constants of a limit-sensitive reaction, $RO_2R\cdot + NO = NO_2 + HO_2\cdot$, reaction 50.

overlapping of other curves shows that the O_3 concentrations are not sensitive to the change of rate constants near the base case rate constant value.

The reasons behind the limit sensitivity of some reactions could be complicated considering the interactions of various reaction pathways. One explanation for the limit sensitivity is that with its base case rate constant, a reaction is so much faster than competing reactions that its dominance is maintained until the rate constant is reduced significantly. For example, Reaction 2, $O + O_2 + M = O_3 + M$, dominates the consumption of O and converts O to O_3. The reaction is very fast, and competing reaction pathways for O do not become important unless the rate constant of Reaction 2 is reduced substantially. Under these conditions, O_3 production due to Reaction 2 would be greatly reduced.

3.2.3. *Non-sensitive reactions.* When the rate constants of this type of reaction are multiplied by a factor ranging from 0 to 2.0, the changes in O_3 concentrations are negligible. Therefore, uncertainties in these rate constants do not directly affect the modelled daytime ozone concentrations unless the uncertainties are many times bigger than the rate constants themselves.

The non-sensitive reactions are indicated in Table 1 by reaction labels without the letter "G" or "L". They include some non-negligible reactions such as NO_3 reactions and O_3 + olefin reactions, which would be expected to be more important at night. Being listed as non-sensitive reactions only imply that O_3 concentrations are not sensitive to the rate constants of these reactions in our base case scenario for the specific time period. When the mechanism is incorporated into another model or it is used in another region, different meteorology and emissions inventory may affect the sensitivities of calculated concentrations to the rate constants of these reactions.

3.3. *Quantitative sensitivity measures of ozone concentrations to the rate constants of sensitive reactions*

Two quantitative measures of sensitivity are calculated for the rate constants of sensitive reactions. They are the sensitivity coefficients based on small rate constant changes, and the effects of large rate constant changes.

3.3.1. *Sensitivity coefficients.* Quantitatively, local sensitivity of maximum O_3 concentration to the ith rate constant can be represented by sensitivity coefficients, defined as

$$\text{sensitivity coefficient} = \frac{\partial(\max O_3)}{\partial k_i} \qquad (1)$$

where $\max O_3$ stands for the maximum 1 h average O_3 concentration and k_i is the base case rate constant of the ith reaction.

For practical purposes, an alternative equation

$$\text{sensitivity coefficient} = \frac{\Delta(\max O_3)}{\Delta k_i/k_i \times 100} \qquad (2)$$

is used and $\Delta k_i/k_i$ is chosen to be

$$\frac{\Delta k_i}{k_i} = \frac{k_i \times 1.1 - k_i \times 0.9}{k_i} = 0.2.$$

Note that the sensitivity coefficient based on equation (2) has a unit ppb O_3 per % k_i, which shows change in maximum 1 h average O_3 in ppb for each percentage change in the rate constant. To implement equation (2), each base case rate constant is multiplied by 0.9 and 1.1 separately and tests are conducted using these modified values. The sensitivity coefficients calculated this way reflect average sensitivity of ozone concentrations to rate constants within the rate constant range $0.9 \times k_i$ to $1.1 \times k_i$, which is close to base case values. The sensitivity coefficients can also be expressed as percentage changes in maximum 1 h average O_3 for each percentage change in the rate constant. The units are then % O_3 per % k_i.

The left half of Table 3 lists sensitivity coefficients for the 44 sensitive reactions in the CD2273V2 mechanism. They are sorted in descending order. The rate constants that have most positive sensitivity coefficients appear at the beginning of the list while those with most negative sensitivity coefficients appear at the bottom. For the convenience of the readers, reactants of the reactions are listed in the right of the table. If multiple pathways exist for the reactants, products of the reactions are also given.

The first three rate constants in the list correspond to photolysis reactions, which are the photolysis of NO_2, HCHO and O_3, respectively. This fact confirms the great sensitivity of O_3 levels to actinic flux, absorption cross-sections and quantum yields which are used to calculate photolysis rates. Uncertainties in these quantities could contribute significantly to uncertainties in calculated O_3 levels. Among the three reactions, NO_2 photolysis has been discussed above. The sensitive HCHO photolysis pathway produces two $HO_2\cdot$ radicals, which then can convert NO to NO_2 and produce $\cdot$OH radicals via Reaction 26, another sensitive reaction. The sensitive O_3 photolysis pathway converts one O_3 molecule to one excited state $O(^1D)$, which then combines with one H_2O molecule to produce two $\cdot$OH via the next sensitive Reaction 17. The loss of one O_3 in the photolysis reaction is more than offset by the production of two $\cdot$OH which accelerate oxidation of NO later in the process. The fifth most sensitive reaction is Reaction 126, which is the lumped reaction ARO2 + OH. As we found in another study (Jiang *et al.*, 1996), calculated O_3 levels in the LFV are greatly affected by the ARO2 emissions. The influences from both the ARO2 emissions and the rate constant are all related to the overall rate of the lumped ARO2 + OH reaction. The uncertainties in the chemistry of aromatics would therefore lead to relatively large uncertainties in calculated O_3 levels.

Three reactions that most negatively affect O_3 levels include the reactions NO_2 + OH, NO + O_3 and the conversion of $O(^1D)$ to ground level $O(^3P)$.

Table 3. O_3 sensitivity to rate constants in the CD2273V2 mechanism

	Sensitivity coefficients		Δ Max O_3 (ppb) if			
k(i)	ppbO_3 per % $k(i)$	% O_3 per % $k(i)$	$k(i)\times 0$	$k(i)\times 0.5$	$k(i)\times 2$	Reactants (= products)
k(1)	0.320	0.493	− 47.3	− 19.0	26.3	$NO_2 + h\nu$
k(68)	0.240	0.370	− 25.9	− 12.9	24.0	HCHO + $h\nu$ (= 2*HO_2 + CO)
k(16)	0.195	0.300	− 18.1	− 9.3	20.9	$O_3 + h\nu$ (= O1D + O_2)
k(17)	0.180	0.277	− 18.3	− 8.9	17.0	O1D + H_2O
k(126)	0.180	0.277	− 29.8	− 12.3	9.8	ARO2 + OH
k(109)	0.090	0.139	− 10.4	− 4.6	7.1	ETHE + OH
k(107)	0.080	0.123	− 9.1	− 4.3	7.3	ALK1 + OH
k(24)	0.075	0.116	− 7.6	− 4.1	7.8	CO + OH
k(84)	0.070	0.108	− 32.1	− 5.7	4.2	C_2O_3 + NO
k(79)	0.065	0.100	− 8.3	− 3.8	6.6	RCHO + $h\nu$
k(89)	0.062	0.095	− 18.7	− 4.9	4.1	PAN
k(125)	0.060	0.092	− 6.8	− 3.1	5.4	ARO1 + OH
k(98)	0.055	0.085	− 10.8	− 3.4	3.6	MGLY + $h\nu$ (= HO_2 + CO + C_2O_3)
k(105)	0.050	0.077	− 21.1	− 3.9	3.0	AFG2 + $h\nu$
k(75)	0.045	0.069	− 6.7	− 2.6	3.5	CCHO + OH
k(113)	0.045	0.069	− 8.8	− 2.7	2.6	OLE1 + OH
k(90)	0.040	0.062	− 13.6	− 2.5	1.6	C_3O_3 + NO
k(76)	0.040	0.062	− 3.7	− 1.8	3.6	CCHO + $h\nu$
k(108)	0.040	0.062	− 6.0	− 2.3	2.6	ALK2 + OH
k(94)	0.030	0.046	− 7.9	− 2.2	2.0	PPN
k(121)	0.020	0.031	− 2.7	− 0.9	0.7	OLE3 + OH
k(118)	0.020	0.031	− 4.5	− 1.4	1.6	OLE2 + O_3
k(82)	0.015	0.023	− 1.3	− 0.6	1.3	MEK + $h\nu$
k(106)	0.015	0.023	− 0.8	− 0.4	1.0	CH_4 + OH
k(20)	0.010	0.015	− 12.3	− 0.6	0.3	HONO + $h\nu$
k(81)	0.010	0.015	− 1.0	− 0.5	1.0	MEK + OH
k(50)	0.010	0.015	− 46.5	0.1	0.0	RO_2R + NO
k(26)	0.005	0.008	− 46.5	− 0.7	0.3	NO + HO_2
k(95)	0.005	0.008	− 1.3	− 0.4	0.4	CRES + OH
k(130)	0.005	0.008	− 2.3	− 0.6	0.3	ISOP + OH
k(2)	0.000	0.000	− 53.8	− 0.3	0.1	O + O_2 + M
k(28)	0.000	0.000	− 34.0	− 0.1	0.2	HNO_4
k(55)	0.000	0.000	− 5.1	0.0	0.0	RO_2N + NO
k(60)	0.000	0.000	− 18.4	0.0	0.0	R_2O_2 + NO
k(131)	0.000	0.000	− 8.0	0.1	0.0	ISOH + NO
k(99)	− 0.015	− 0.023	1.9	0.8	− 1.2	MGLY + OH
k(104)	− 0.015	− 0.023	2.0	0.8	− 1.5	AFG2 + OH
k(70)	− 0.025	− 0.039	2.8	1.3	− 2.0	HCHO + OH
k(91)	− 0.030	− 0.046	3.9	1.8	− 2.4	C_3O_3 + NO_2
k(69)	− 0.070	− 0.108	8.8	3.7	− 5.5	HCHO + $h\nu$ (= CO)
k(85)	− 0.085	− 0.131	10.0	4.3	− 5.8	C_2O_3 + NO_2
k(18)	− 0.170	− 0.262	45.1	17.2	− 8.9	O1D + M
k(5)	− 0.305	− 0.470	343.1	25.7	− 18.8	NO + O_3
k(21)	− 0.588	− 0.903	164.7	43.7	− 33.4	NO_2 + OH

They are Reactions 21, 5 and 18, respectively. Loss of O_3 by the NO + O_3 reaction is very obvious. Loss of $O(^1D)$ by Reaction 18 reduces the system's ·OH production ability and indirectly makes the O_3 concentrations lower. Negative O_3 sensitivity of the NO_2 + OH reaction in our LFV modelling system is mostly caused by the consumption of ·OH instead of the consumption of NO_2 by the reaction. Our other studies show that increasing NO_2 emissions leads to lower O_3 concentrations in the Vancouver urban plume (Jiang *et al.*, 1996). Combining that fact with the negative sensitivity of the NO_2 + OH rate constant, it can be concluded that the consumption of ·OH by the NO_2 + OH reaction is responsible for decreased O_3 levels.

An important condition that could affect the values of sensitivity coefficients is the amount of NO_x emissions. To see the potential impact of NO_x emissions, we calculated sensitivity coefficients for a scenario in which NO_x is reduced by 60%, which corresponds to the NO_x level for maximum ozone in the scenario. Qualitatively, we found that the grouping of sensitive and non-sensitive reactions remained the same for the lower NO_x scenario with a few minor exceptions. In general, the sensitivity coefficients were smaller for the lower NO_x scenario. For the most positively and negatively sensitive reactions in Table 3, the sensitivity coefficients of $NO_2 + h\nu$, NO + O_3 and C_2O_3 + NO_2 were 82, 71 and 84%, respectively, of the values in the high NO_x scenario. The sensitivity

coefficients of Reactions 68, 16, 17, and 126 and 21, 18, and 69 were 17–30% of the values in the high NO_x scenario. For other reactions involving NO or NO_2, there tended to be much smaller or virtually no changes in sensitivity coefficients, with the exception of Reaction 26, $HO_2 + NO = OH + NO_2$, for which the sensitivity increased from 0.008 to 0.096% O_3 per $\%k_{26}$ in the low NO_x scenario. This difference in the sensitivity of the reactions of NO and NO_2 is probably related to the system moving towards conditions where availability of NO_x is becoming more important in the low NO_x scenario.

3.3.2. *Effects of large rate constant changes.* Sensitivity coefficients calculated above can be considered as a sensitivity measurement for small rate constant changes near the base case situation. When a rate constant is changed far enough from its base case value, the effect on O_3 concentrations can be different from that indicated by the sensitivity coefficient. The middle part of Table 3 lists changes in maximum 1 h average O_3 concentrations when the base case rate constants of the sensitive reactions are multiplied by 0, 0.5, and 2. They can be used as a supplement to the sensitivity coefficients in assessing impact of changed rate constants to O_3 levels. Note that reactions in Table 3 are sorted in descending order of sensitivity coefficients. The order for effects of large changes in rate constant is not necessarily the same.

4. DISCUSSION AND CONCLUSIONS

We modified and updated a version of the SAPRC90 mechanism implemented in CALGRID using LFV emissions profiles, more recent experimental results and newly recommended rate constants. The new CD2273V2 mechanism contains explicit reactions for modelling impacts of alternative fuels and biogenic emissions, and will be used in both the OZIPR trajectory model and the CALGRID model to evaluate the potential roles of these emissions on air quality in the LFV.

Sensitivity of ozone concentrations to rate constants of the new mechanism was determined using the OZIPR trajectory model for conditions of an ozone episode in the LFV. The adopted trajectory simulated the daytime chemistry of an urban plume in the LFV. Out of the 137 reactions in the mechanism, 44 reactions were classified as sensitive reactions. Among them, 36 are general sensitive reactions. The other eight reactions were designated as limit-sensitive reactions since they only become sensitive when their rate constants approach the limit of zero or the rate constants are reduced by more than an order of magnitude. The remaining 93 reactions in the mechanism were not sensitive when their rate constants were changed from zero to two times their base case values.

In general, the reactions identified as most sensitive to ozone formation in this work are consistent with the results of other recent studies involving several chemical mechanisms (Yang *et al.*, 1995; Gao *et al.*, 1995; Dechaux *et al.*, 1994). The objective of these studies was to determine the influence of estimated uncertainties in kinetic parameters on calculated concentrations of ozone and other model species. If the rate constant sensitivities to ozone formation reported for the RADM2 (Gao *et al.*, 1995) and the SAPRC90 (Yang *et al.*, 1995) mechanisms are adjusted assuming constant fractional uncertainty in the rate constants, the most sensitive reactions identified in these studies are consistent with the present results. The exceptions are some photolytic radical generation reactions in the RADM2 mechanism that are less sensitive than found in the present study. Examples are photolysis of O_3 and aldehydes, and reactions of $O(^1D)$. This may be due to the use of higher initial concentrations in the RADM2 study, with no subsequent emissions. Very low initial concentrations of ozone and its precursors would make the system more sensitive to radical generation processes. This result illustrates a significant difference for the LFV compared to the typical situation in eastern North America in which long range transport of O_3 and its precursors leads to high initial concentrations in the analysis of sub-regional air quality.

The explicit reactions of components of alternative fuels, such as propane, methanol, ethanol, and MTBE were not identified as sensitive reactions. This is likely due to the low emission rate of these species under the present scenario combined with the relatively small rate constants for the reactions of these species with OH. However, it is expected that the importance of these reactions could increase in future year scenarios that involve significant application of technologies utilizing these fuels.

In usual applications of trajectory models, the trajectory is selected based on the final destination of an air mass. The destination is selected to coincide with the location of a monitoring station so that final calculated concentrations can be compared with observations. In the present work, the trajectory was selected to track an air mass that passed over the urban core during the morning rush hour. The trajectory therefore represents a situation where the air mass receives maximum early morning emissions during an actual ozone episode. Since the focus of this paper is to study the sensitivity of ozone concentrations to rate constants in order to characterize the modelling system, no attempt is made to adjust either base case emissions or other conditions in order to match the calculated concentrations with the ambient measurement data.

However, the underprediction of ozone concentrations by the model is obvious for the adopted modelling conditions. The calculated maximum 1 h average O_3 concentration along the trajectory is 64.9 ppb when the base case rate constants are used. The value is 37% lower than the peak value of 102.5 ppb measured at a downwind station at Chilliwack on 18 July 1995. Although the comparison is not expected to be

accurate due to the 25 km distance between the Chilliwack station and the selected trajectory, such a large gradient in ozone concentrations this far downwind is not expected. It is reasonable to conclude that there is an underprediction of O_3 concentrations. The lower calculated peak O_3 concentrations are caused in part by a too rapid decrease in morning O_3 concentrations, from 8:00 to 10:00 a.m., due to NO_x titration of O_3 in the model calculation. Such low values of O_3 concentrations were not observed in the nearby urban monitoring stations in the morning hours. Although better agreement with observed ozone concentrations could be obtained by adjustments to the emissions or initial conditions, there is no independent justification for doing so. Uncertainties in the chemical mechanism could also contribute to the underestimation of ozone, and the sensitivity study in this work identifies the most critical groups of reactions.

The present study focused on a trajectory that includes the peak morning emissions from the urban core of Vancouver. The sensitivity of ozone concentrations in the LFV to either kinetic parameters or emissions is expected to have a spatial variability that could only be estimated by using a 3D model, a process that would require significantly more resources. Also, the simulation was conducted only for daylight hours, and the influence of nighttime chemistry was not evaluated. Within these limitations, the present study provides a basis for identifying areas for further study. For example, the sensitivity of the rate constants of several photolysis reactions on O_3 formation indicates that uncertainties in absorption cross sections, quantum yields and actinic fluxes could have substantial impact on model performance. Also, uncertainties in the chemistry of aromatics can have a significant impact, since the sensitivity of ozone concentrations to the rate constant of the ARO2 + OH reaction is very high. In another study concerning emissions in the LFV (Jiang *et al.*, 1996), we also found that the ozone concentrations in the LFV are very sensitive to the ARO2 emissions in the valley. Future work with the MC2-CALGRID model will evaluate this sensitivity more fully. Although the modelling studies indicate the importance of the chemistry of aromatics in the LFV, the chemistry of these compounds is one of the more uncertain areas in chemical mechanisms used in photochemical models. Therefore, the aromatic chemistry should be a priority to be addressed in future research.

Acknowledgements—The authors would like to thank Dr William P. L. Carter at University of California, Riverside, Dr Fred Lurmann and Dr Naresh Kumar at STI for their timely help in implementing Carter's mechanism preparation package. Special thanks are also extended to Dr Neil Wheeler, Dr Donald Johnson and Bart Croes at the California Air Resources Board for their software and documentation support. Ms Susan Bohme and Mr Alfred Dorkalam helped process the emissions inventory and provided technical assistance to the project. Their contribution is deeply appreciated.

This project is supported by Natural Resources Canada and the National Research Council of Canada.

REFERENCES

Aschmann S. M. and Atkinson R. (1994) Formation yields of methyl vinyl ketone and methacrolein from the gas-phase reaction of O_3 with isoprene. *Envir. Sci. Technol.* **28,** 1539–1542.

Atkinson R. (1994) Gas-phase tropospheric chemistry of organic compounds. *J. Phys. Chem. Ref. Data*, Monograph No. 2.

Carter W. P. L. (1988) Documentation for the SAPRC atmospheric photochemical mechanism preparation and emissions processing programs for implementation in airshed models. Prepared for the California Air Resources Board Contract No. A5-122-32. Statewide Air Pollution Research Centre, University of California, Riverside, California.

Carter W. P. L. (1990) A detailed mechanism for the gas-phase atmospheric reactions of organic compounds. *Atmospheric Environment* **24A,** 481–518.

CCME (1990) Management plan for nitrogen oxides (NO_x) and volatile organic compounds (VOCs) Phase I. Canadian Council of Ministers of the Environment.

Chameides W. L., Fehsenfeld F., Rodgers M. O., Cardelino C., Martinez J., Parrish D., Lonneman W., Lawson D. R., Rasmussen R. A., Zimmerman P., Greenberg J., Middleton P. and Wang T. (1992) Ozone precursor relationships in the ambient atmosphere. *J. geophys. Res.* **97,** 6037–6055.

Dann T., Wang D., Steenkamer A., Halman R. and Lister M. (1994) VOC measurements in the Greater Vancouver Regional District, 1989–1992. Environment Canada, Ottawa, Ontario PMD 94-1.

Dechaux J. C., Zimmermann V. and Nollet V. (1994) Sensitivity analysis of the requirements of rate coefficients for the operational models of photochemical oxidants formation in the troposphere. *Atmospheric Environment* **28,** 195–211.

Finlayson-Pitts B. J. and Pitts J. N. Jr. (1986) *Atmospheric Chemistry: Fundamentals and Experimental Techniques.* J. Wiley, New York

Gao D., Stockwell W. R. and Milford J. B. (1995) First-order sensitivity and uncertainty for a regional-scale gas-phase chemical mechanism. *J. geophys. Res.* **100,** 23,153–23,166.

Gardner L., Causley M., Wilson G. and Jimenez M. (1992) User's Guide for the urban airshed model, Volume IV. *User's Manual for the Emissions Preprocessor System* 2.0. U.S. Environmental Protection Agency, Research Triangle Park, North Carolina.

Gery M. W. and Crouse R. R. (1989) *User's Guide for Executing OZIPR.* Atmospheric Research and Exposure Assessment Laboratory, U.S. Environmental Protection Agency, Research Triangle Park, North Carolina.

Grosjean D., Williams II E. L. and Grosjean E. (1993) Atmospheric chemistry of isoprene and of its carbonyl products. *Envir. Sci. Technol.* **27,** 830–840.

Jiang W., Singleton D. L., Hedley M. and McLaren R. (1995) Modification and evaluation of the CALGRID chemical mechanism for ozone studies of the Lower Fraser Valley, B.C. Report No. PET-1360-95S, National Research Council Canada.

Jiang W., Singleton D. L., Hedley M. and McLaren R. (1996) Sensitivity of ozone concentrations to VOC and NO_x emissions in the Canadian Lower Fraser Valley. *Atmospheric Environment* **31,** 627–638.

McLaren R., Bohme S., Hedley M., Jiang W., Dorkalam A. and Singleton D. L. (1995) Emissions inventory processing for UAM-V and CALGRID modelling in the Lower Fraser Valley. *Proc. Int. Symp., The Emissions Inventory: Programs and Progress,* Vol. VIP56, pp. 749–764. Air & Waste Management Association.

NRC (National Research Council) (1991) *Rethinking the Ozone Problem in Urban and Regional Air Pollution.* National Academy Press, Washington, District of Columbia.

Paulson S. E. and Seinfeld J. H. (1992) Development and evaluation of a photooxidation mechanism for isoprene. *J. geophys. Res.* **97,** 20,703–20,715.

Paulson S. E., Flagan R. C. and Seinfeld J. H. (1992a) Atmospheric photooxidation of isoprene Part I. The hydroxyl radical and ground state atomic oxygen reactions. *Int. J. Chem. Kinet.* **24,** 79–101.

Paulson S. E., Flagan R. C. and Seinfeld J. H. (1992b) Atmospheric photooxidation of isoprene Part II. The ozone-isoprene reaction. *Int. J. Chem. Kinet.* **24,** 103–125.

Scire J. S., Yamartino R. J., Carmichael G. R. and Chang Y. S. (1989) CALGRID. A mesoscale photochemical grid model. Volume II. User's Guide. California Air Resources Board, Sacramento, California.

Tanguay M., Robert A. and Laprise R. (1990) A Semi-implicit Semi-lagrangian Fully Compressible Regional Forecast Model. *Mon. Weath. Rev.* **118,** 1970–1980.

Tuazon E. C. and Atkinson R. (1989) A product study of the gas-phase reaction of methyl vinyl ketone with the OH radical in the presence on NO_x. *Int. J. Chem. Kinet.* **21,** 1141–1152.

Tuazon E. C. and Atkinson R. (1990) A product study of the gas-phase reaction of methacrolein with the OH radical in the presence of NO_x. *Int. J. Chem. Kinet.* **22,** 591–602.

Yamartino R. J., Scire J. S., Carmichael G. R. and Chang Y. S. (1992) The CALGRID mesoscale photochemical grid model—I. Model formulation. *Atmospheric Environment* **26A,** 1493–1512.

Yang Y., Stockwell W. R. and Milford J. B. (1995) Uncertainties in incremental reactivities of volatile organic compounds. *Envir. Sci. Technol.* **29,** 1336–1345.